https://doi.org/10.1590/jatm.v18.1449

ORIGINAL PAPER

Numerical Simulations of Nanosatellite Dynamics for the Assessment of Hysteresis Rod Damping in Very Low Earth Orbits

Tirza Ohana Berger de Souza[1,*], Igor Andreevich Lomaka[1]

1.Samara National Research University – Interuniversity Department of Space Research – Samara – Russia.

*Corresponding author: ohanabergerr@gmail.com

ABSTRACT

Over the past decade, nanosatellites have evolved from simple educational platforms into effective tools for scientific research, technology demonstration, and commercial services. This growth resulted in a sharp increase in deployments in Low Earth Orbit (LEO), contributing to its congestion. Very Low Earth Orbits (VLEO), typically below 400 km, are therefore becoming an attractive alternative. Their proximity to Earth offers advantages such as improved sensing performance and reduced communication latency, but also introduces significant challenges due to the strong aerodynamic resistance in the denser atmospheric layers. A particular feature of VLEO is the stronger interaction with Earth's geomagnetic field compared to LEO, suggesting that passive magnetic attitude control (PMAC) may be effective in this regime. Therefore, this paper presents numerical simulations, based on a methodology developed at Samara University, to assess angular-velocity damping using soft magnetic materials in VLEO. The simulations account for spacecraft-specific parameters, mission requirements, and different possible configurations. The methodology is described in sufficient detail to allow reproduction, providing a practical tool for early mission design.

Keywords: Nanosatellites; Attitude control; Magnetic damping; Hysteresis.

INTRODUCTION

Very Low Earth Orbits (VLEO), typically defined as circular orbits below 400 km, have attracted increasing interest in recent years due to several advantages. The reduced altitude improves spatial resolution for Earth-observation missions, enhances communication links due to shorter signal paths, lowers latency, and enables faster natural deorbiting that contributes to space-debris mitigation (Crisp *et al.* 2021). Additionally, as the number of small satellites has increased rapidly in the past decade, traditional Low Earth Orbit (LEO) has become progressively congested, making VLEO an attractive alternative for future constellations and research missions.

Spacecraft operating in this region, however, face technical challenges, the most significant being the high atmospheric density, which leads to increased aerodynamic drag, accelerated surface degradation, and reduced orbital lifetime. These factors complicate mission design and have historically restricted long-term operations in VLEO or required large, power-intensive attitude-control systems, as seen in missions such as GOCE (Allasio *et al.* 2010) and SLATS (Walsh *et al.* 2021). This represents an important limitation for small satellites, since such control techniques are often incompatible with constraints on mass, volume, cost,

Received: Nov. 17, 2025 | **Accepted:** May 16, 2026
Peer Review History: Single Blind Peer Review.
Section editor: Luiz Martins-Filho

and power. While numerous CubeSats deployed from the International Space Station naturally decayed into VLEO, they were not originally designed for sustained operation at such altitudes or to specifically exploit the benefits of closer proximity to Earth.

One aspect of these lower altitudes that remains relatively underexplored is the stronger interaction with Earth's magnetic field. As the spacecraft approaches Earth, the geomagnetic field intensity increases, suggesting that magnetic materials could be installed onboard and used for attitude control. However, to date, no missions have relied exclusively on passive magnetic stabilization at altitudes below 300 km. One possible explanation is that VLEO has traditionally been used either by large spacecraft requiring robust and responsive control systems or, more recently, by small satellites whose development efforts have focused primarily on drag compensation and aerodynamic shaping rather than magnetic stabilization.

Motivated by this gap, the present study assesses the feasibility of using hysteresis materials to passively damp angular oscillations of nanosatellites operating in VLEO. The analysis builds on a methodology developed at the Department of Space Research at Samara University to provide passive magnetic attitude control (PMAC) for small spacecraft in LEO. Although the original methodology accounts for the presence of permanent magnets, this paper focuses exclusively on the damping of angular velocities using hysteresis rods, and no permanent magnets were included in the simulated configurations.

This paper is organized as follows: the first section provides the background for this work, including an overview of passive attitude control systems, the principles of magnetic hysteresis, the main design challenges, and the methodology developed in this study to provide PMAC, together with its implementation in dedicated software. The following section discusses the VLEO environment in terms of atmospheric density and Earth's magnetic field, and their effect on the attitude behavior of small satellites. Then, the attitude dynamics model is presented, including the equations of motion used in the simulations. The final section reports and discusses the numerical results obtained for different PMAC configurations.

Background

Passive attitude control systems

With the growing use of nanosatellite platforms, missions have become more sophisticated and so have the performance requirements placed on them. Most missions demand specific pointing and stabilization of angular velocities, and attitude control systems ensure that payloads, sensors, and communication equipment maintain their intended orientation. Active control techniques, such as reaction wheels and magnetorquers, are programmed to generate torques that counteract the maximum expected disturbance torques along the orbit (Rawashdeh 2010). They offer fast response times and high pointing accuracy, with studies reporting body-pointing precision on the order of 20 milliarcseconds (Douglas *et al.* 2021). For small satellites like CubeSats, these factors become particularly critical: the restricted mass, volume, and energy budgets limit the inclusion of redundant actuators or high-power subsystems, and the low-cost philosophy behind many small-satellite missions makes active systems less attractive economically.

Passive attitude control methods, on the other hand, take advantage of the natural torques acting on a satellite during orbital motion and are appealing for nanosatellites because they require little to no energy or volume (Belokonov *et al.* 2019). For small spacecraft in LEO, the most relevant passive mechanisms include aerodynamic stabilization, arising from the torque generated by atmospheric flow acting on an offset between the center of pressure and the center of mass; gravity-gradient stabilization, which results from the varying gravitational force across the satellite's mass distribution; and magnetic stabilization, which relies on interactions between onboard magnetic materials and Earth's magnetic field.

Among the cited passive techniques, leveraging the interaction between magnetic materials installed onboard the spacecraft and the geomagnetic field has proven effective in several missions across LEO altitudes (Carletta *et al.* 2022; Ovchinnikov and Penkov 2010; Santoni *et al.* 2009). This approach, known as passive magnetic attitude control (PMAC), typically combines two types of magnetic materials: (1) permanent (hard) magnets, which align one of the spacecraft axes with Earth's magnetic field lines; (2) soft magnetic materials, such as hysteresis rods, which damp angular motion by dissipating rotational kinetic energy as heat.

Design challenges

One of the main drawbacks of passive attitude control systems, when compared to active solutions, is that their performance is fully determined during the design phase (Belokonov *et al.* 2019). As the control authority cannot be modified once in orbit, the spacecraft's attitude behavior will directly reflect the accuracy of the modelling assumptions and design parameters adopted during the design phase. As a result, accurately predicting the orbital and attitude behavior becomes a critical step in ensuring that the system will operate as intended. Passive magnetic attitude control (PMAC) introduces an additional layer of complexity: although the overall concept is simple, modelling the actual behavior of soft magnetic materials during orbital motion is far from trivial (Ovchinnikov 2012; Santoni *et al.* 2009).

In addition to the inherently nonlinear magnetic response, the effectiveness of hysteresis rods depends on a large number of factors. These include rod volume and aspect ratio, material properties, onboard placement, relative orientation, and even manufacturing details such as heat treatment (Battagliere *et al.* 2010). Small variations in these parameters can lead to significant differences in stabilization performance. Table 1 presents a summary of nanosatellite missions employing PMAC, together with the time required to achieve stabilization (Aslan *et al.* 2011; Carletta *et al.* 2022; Farrahi and Sanz-Andrés 2013; Gerhardt 2010). The last column reports the stabilization time, defined here as the time after which the angular oscillations fall within the acceptable range specified for each mission. Although this range varies between missions, it typically lies within ±10–15 $degs^{-1}$.

Table 1. PMAC configurations used in previous nanosatellite missions.

Mission	Initial angular velocities	Hysteresis rod (material, length × width)	Number of rods	Permanent magnet (quantity, dipole moment)	Stabilization time (days)
CSSWE (3U)	[10, 5, 5] $deg \cdot s^{-1}$	HyMu-80, 95 × 1 mm	2	1 magnet, 0.3 $A \cdot m^{-2}$	~ 7
Astrobio (3U)	Randomly selected in the range ± 2.5 $deg \cdot s^{-1}$	EFI Alloy 79, 65 × 0.5 mm	4	4 magnets, 0.3 $A \cdot m^{-2}$	~ 1
TURKSAT (3U)	In the ±15 $deg \cdot s^{-1}$ range	HyMu-80, 80 × 1 mm	6	1 magnet, 0.3 $A \cdot m^{-2}$ (for 10 accuracy)	Not available
DELFI-3C (3U)	Not informed	Mo-Permalloy, 70 × 11 mm (circular cross-section)	2	1 magnet, 0.3 $A \cdot m^{-2}$	~ 30

Source: Elaborated by the authors.

The variability in these configurations suggests that there is no single optimal design; rather, many different combinations can lead to a functioning PMAC system. Although previous studies have investigated different configurations and demonstrated their effectiveness, the design criteria used to select specific parameter combinations are not always explicitly formulated or easily generalized. This can pose a challenge for future research, especially for organizations that do not have access to advanced laboratory facilities to experimentally test magnetic response. In this context, the Department of Space Research at Samara University has developed a methodology for analyzing and selecting PMAC parameters, with the aim of improving predictions of system behavior during orbital motion and supporting researchers in making informed design decisions.

The methodology was previously applied to assess PMAC in LEO (Souza and Lomaka 2024). Building on this methodology, the present study focuses on isolating the damping behavior of hysteresis rods and assessing their effectiveness in stabilizing angular motion within an initial angular-velocity range of ±15 degrees in VLEO.

Methodology for PMAC and software implementation

The developed methodology is designed to model and predict the behavior of nanosatellites in LEO, including VLEO, under the interaction between onboard magnetic materials and the geomagnetic field. It consists of two main components: (1) modelling the orbital motion of the satellite's center of mass; and (2) modelling the attitude dynamics relative to the center of mass. The methodology does not consider the interaction between the hysteresis rods and the permanent magnets.

The process begins with the selection of the initial orbital parameters, including orbit type, altitude, and Keplerian elements. These parameters are converted into Cartesian state vectors, and the satellite's orbital trajectory is propagated numerically. At each time step, the satellite's latitude, longitude, and altitude are obtained from the propagated state. These coordinates serve as inputs to the 13th generation of the International Geomagnetic Reference Field (IGRF-13) model, which provides the magnetic field vector at the spacecraft location for every step of the simulation. The resulting magnetic field time series is then used as an external input for the attitude dynamics model.

The next stage focuses on the rotational motion of the satellite. The attitude model uses the spacecraft's mass and inertia properties, the center-of-mass offset, and the initial attitude and angular velocity components as the main inputs. The initial attitude is specified using Euler angles, which are then converted into quaternions to initialize the attitude state for numerical integration. These quaternions define the rotation matrix used to transform the magnetic field vector (computed in the orbital block) into the body reference frame at each time step.

Since PMAC does not offer a direct analytical mapping between mission requirements and hardware parameters, the design process begins by selecting an initial set of magnetic system inputs. These include preliminary choices of hysteresis-rod material and geometry, an initial estimate of the permanent magnet dipole moment (checked against resonance conditions), and assumptions about the number and arrangement of magnetic elements onboard.

Once the magnetic system is defined, all external torques acting on the spacecraft during orbital motion are computed. The methodology accounts for aerodynamic torque, gravity-gradient torque, and the magnetic torques responsible for alignment (restoring torque) and damping, generated by the permanent magnets and the hysteresis rods, respectively. The magnetic field obtained from the orbital block is used directly to compute these magnetic torques. The simulation then integrates the full set of rotational equations of motion, allowing the evaluation of the angular-velocity damping time and orientation. The methodology is supported by dedicated in-house-developed software that implements the modelling procedure and serves as both an educational and a research tool (Fig. 1).

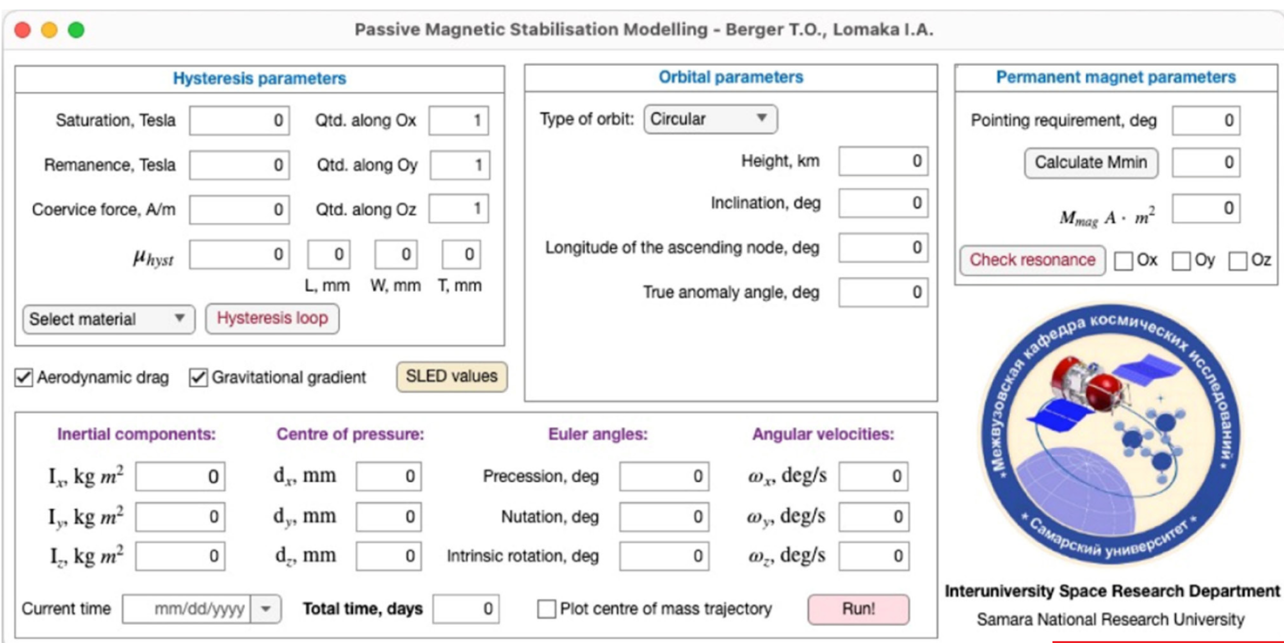

Source: Elaborated by the authors.

Figure 1. Interface of the software implementing the methodology.

Prezada autora
Teria a fig em melhor resolução?

An updated version of the software has been developed and optimized to compare the response of hysteresis-rod damping under different configurations. In this version, two comparison modes are implemented, and permanent magnet parameters are not included. The first mode evaluates different magnetic system configurations for the same spacecraft, including variations in hysteresis-rod material, number, placement, and initial orbital parameters (Fig. 2). The second mode compares the behavior of a fixed magnetic configuration across spacecraft with different inertia properties and center-of-mass offsets (Fig. 3). The results are used to identify which configurations meet the mission's requirements in terms of damping performance before moving to laboratory testing.

To ensure full transparency and control over the numerical calculations, the program includes a custom implementation of the classical fourth-order Runge-Kutta integrator for angular motion, as well as internally developed routines for quaternion operations,

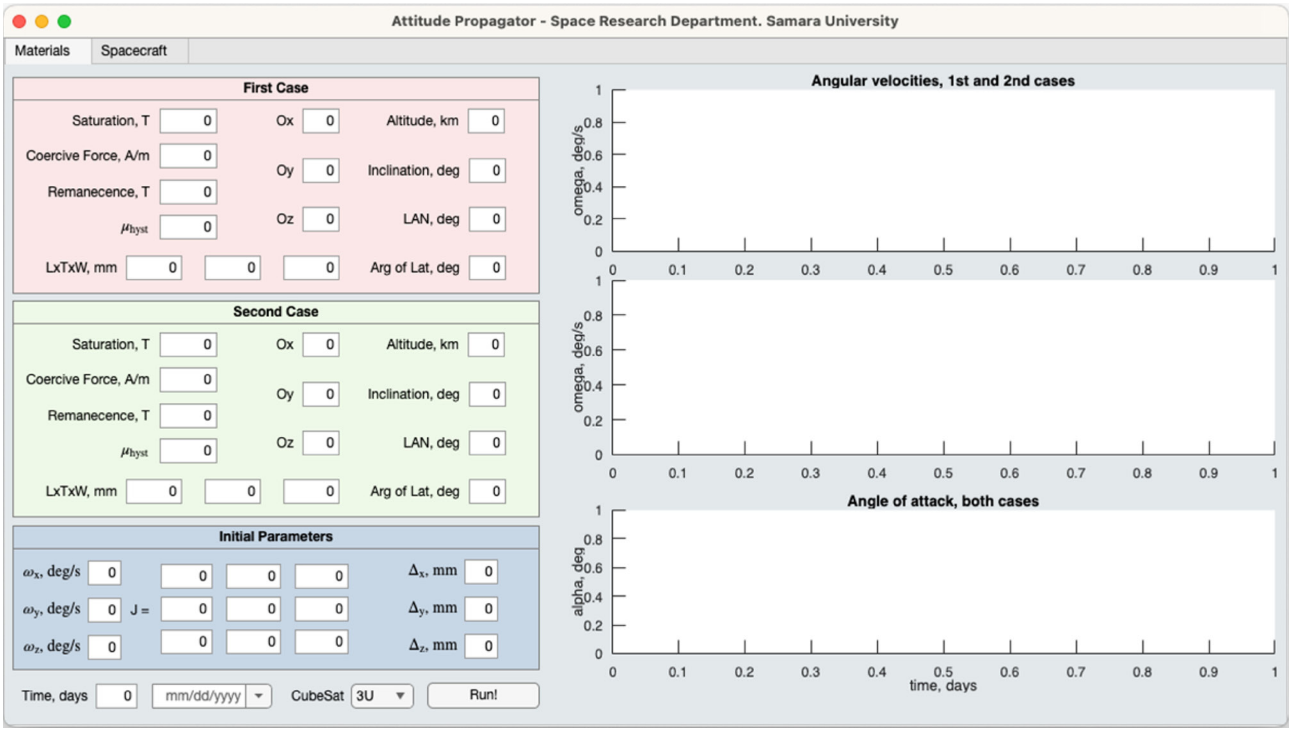

Source: Elaborated by the authors.

Figure 2. First comparison mode of the attitude propagation software.

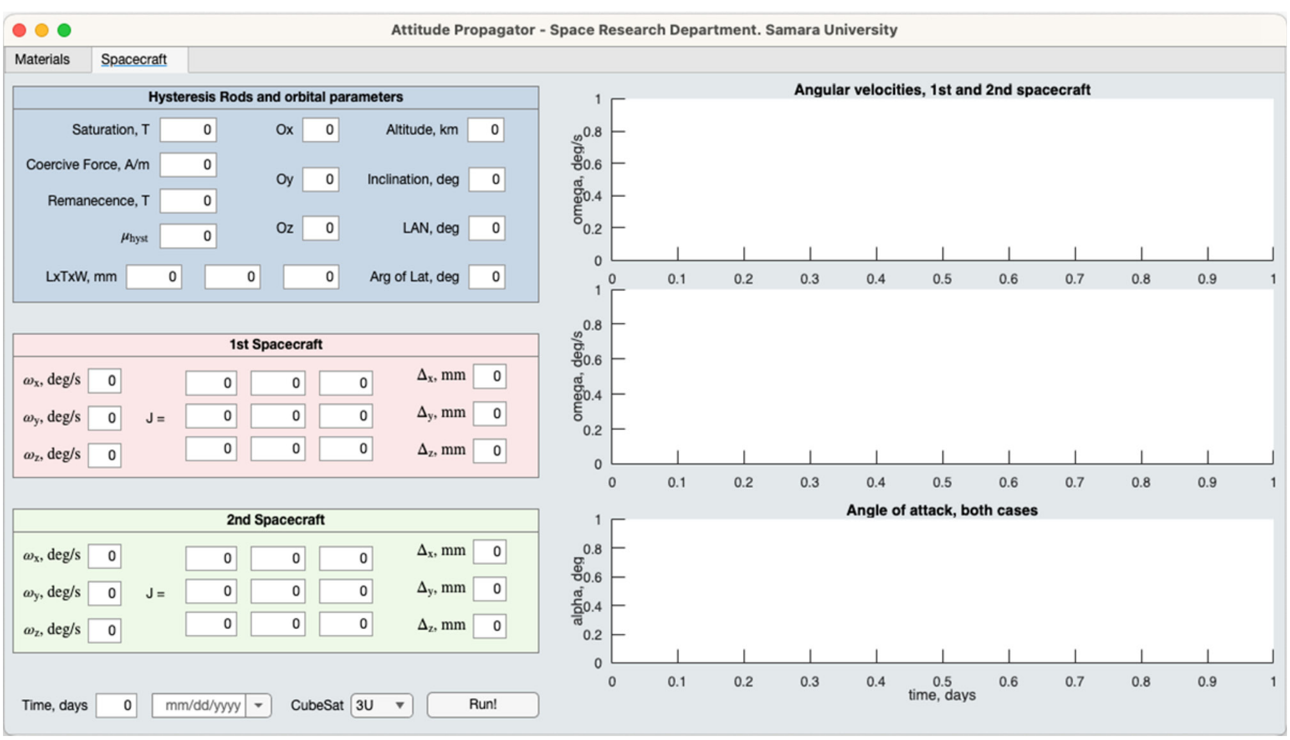

Source: Elaborated by the authors.

Figure 3. Second comparison mode of the attitude propagation software.

reference-frame transformations, and torque computation. The geomagnetic field is calculated using the IGRF-13 model, and atmospheric density is obtained from the empirical NRLMSISE-00 model. The orbital propagator incorporates J2 perturbations.

As all previous missions employing PMAC were originally designed to operate at altitudes above 400 km, they have provided useful insights into desirable design parameters for that altitude range, such as material types, dipole moments, and rod dimensions. However, this limits the applicability of existing design experience to nanosatellites intended to function at lower altitudes, making the methodology and the simulation software suitable tools for assessing passive magnetic techniques in nanosatellites designed to operate in VLEO.

In this context, while the final validation of a PMAC system must be performed experimentally, testing several possible configurations under laboratory conditions is impractical. The software, therefore, provides a first-level estimation of the expected damping behavior and helps to identify promising configurations that comply with mission requirements, particularly in terms of damping time. A graphical representation of the software implementation of the proposed methodology is shown in Fig. 3.

VLEO environment

Operating in VLEO has advantages from both practical and scientific perspectives, which is reflected in the growing interest in the development and study of VLEO missions (Crisp *et al.* 2021; DISCOVERER 2025; Jiang *et al.* 2023; Sizov *et al.* 2024; Walsh *et al.* 2021). From an applied perspective, operating closer to Earth's surface enables improved communication performance, reduced latency, and shorter revisit times for Earth-observation missions (Crisp *et al.* 2021). Lower altitudes also accelerate natural deorbiting, contributing to space-debris mitigation, and may reduce launch and operational costs (BIS Research 2025). Furthermore, VLEO altitudes offer a viable alternative to traditional LEO, whose congestion continues to grow as satellite constellations expand.

From a scientific point of view, missions operating at these altitudes have the potential to provide valuable data on a region of near-Earth space that remains insufficiently characterized. In particular, the lower thermosphere exhibits large uncertainties in existing empirical atmospheric density models, which affects orbit prediction, reentry forecasting, and aerodynamic force estimation (Martinez *et al.* 2022) and could be improved with *in-situ* measurements from spacecraft flying in VLEO.

At the same time, the particularities of these altitudes, most notably the substantially increased atmospheric density, require special care when modelling the angular motion of small spacecraft. In VLEO, aerodynamic forces become strong enough to influence not only orbital decay but also the rotational dynamics. At 300 km, for example, atmospheric density is about six times higher when compared to 600 km. Accurate environmental modelling is then essential for any attitude-stabilization analysis.

Aerodynamic influence on the motion of nanosatellites

For simplification purposes, when modelling the angular motion of spacecraft at higher altitudes, where other external forces dominate, the atmospheric effect is often neglected. However, this approach is not applicable to VLEO, as at these altitudes the effect of aerodynamic drag is significant and may represent the dominant external disturbance acting on the spacecraft. This aerodynamic influence is particularly important for nanosatellites: despite their relatively small cross-sectional area, small spacecraft are highly sensitive to atmospheric drag due to their large area-to-mass ratio, resulting in a higher ballistic coefficient (Belokonov and Timbay 2020):

$$\sigma = \frac{C_x S}{m} \tag{1}$$

where C_x is the drag coefficient, S is the projected cross-sectional area of the nanosatellite perpendicular to the velocity vector of the incoming flow, and m is the satellite's mass. When comparing a 1U CubeSat with linear dimensions of $0.1 \times 0.1 \times 0.1$ m^3 to a microsatellite with dimensions of $1 \times 1 \times 1$ m^3, for example, the relationship can be expressed as:

$$\sigma_c \sim \frac{C_x l^2}{m_c} = \frac{C_x l^2}{\gamma_c l^3} = \frac{C_x}{\gamma_c l}, \sigma_m \sim \frac{C_x L^2}{m_m} = \frac{C_x L^2}{\gamma_m L^3} = \frac{C_x}{\gamma_m L} \tag{2}$$

where γ_c, m_c, l represent the volumetric density, mass, and edge length of the CubeSat, and γ_m, m_m, L are the corresponding values for the microsatellite. From the expressions in Eq. 2, the ratio between the ballistic coefficients of the CubeSat and the microsatellite is given by:

$$\frac{\sigma_{\text{с}}}{\sigma_{\text{б}}} = \frac{\gamma_{\text{б}} L}{\gamma_{\text{м}} l} = 10\,\frac{\gamma_{\text{м}}}{\gamma_{\text{б}}} \tag{3}$$

The orbital lifetime of a satellite is primarily determined by the rate at which atmospheric drag causes the orbit to decay. While its precise prediction requires numerical integration, an inverse proportionality can be established (Afful 2014):

$$T_{orb} \propto \frac{1}{\rho \cdot \sigma} \tag{4}$$

where ρ is the atmospheric density at a given orbital altitude. It follows that the higher the ballistic coefficient σ, the faster the orbit decays. Thus, accounting for aerodynamic drag is not only essential for accurately modelling the dynamics of satellites in VLEO but becomes especially critical when performing calculations for nanosatellites.

The atmospheric density model also plays an important role in the simulations. In practice, simplified static models, such as the Russian standard atmosphere model GOST 4401-81, are often used for convenience, at the cost of accuracy. More accurate and high-fidelity models exist, but they add extra computational complexity. This work uses the NRLMSISE-00 model, which is commonly used in simulations of spacecraft operating in VLEO (Romano *et al.* 2021) and offers a good balance between accuracy and complexity (Virgili-Llop *et al.* 2019).

Interaction with the geomagnetic field

In VLEO, a spacecraft operates not only in a denser atmospheric environment but also closer to Earth's surface, where the geomagnetic field is moderately stronger than at higher altitudes. For simplified analysis, the magnetic field can be approximated using the ideal dipole model, in which the magnetic field strength B is inversely proportional to the cube of the distance from Earth's center.

This approach, however, may overestimate magnetic torques and oscillation damping, leading to inaccurate predictions. Since the intensity of the geomagnetic field experienced by the spacecraft depends on altitude, time, geographic location, and solar–geomagnetic activity, accurate modelling requires the use of reliable empirical models. In this work, Earth's magnetic field is computed using the IGRF-13 model.

Attitude dynamics modelling

Equations of motion and numerical integration

The rotational motion of the spacecraft is described using quaternions according to the following set of differential equations:

$$\dot{q} = \frac{1}{2}\Omega(\omega_{rel})q \tag{5}$$

$$\dot{\omega} = I^{-1}(-\omega \times (I\omega) + T_{\Sigma}) \tag{6}$$

where $q = [q_0 \quad q_1 \quad q_2 \quad q_3]^T$ is the quaternion describing the orientation of the spacecraft body frame with respect to the orbital frame, ω is the angular velocity of the spacecraft in the body frame, and T_{Σ} is the total external torque acting on the spacecraft.

The total external torque is defined as:

$$T_{\Sigma} = T_a + T_{grav} + T_{mag-damp} \tag{7}$$

which corresponds to the sum of the aerodynamic torque, the gravity-gradient torque, and the magnetic damping torque generated by hysteresis rods, respectively.

The relative angular velocity is given by:

$$\omega_{rel} = \omega - C\omega_{orb} \tag{8}$$

where C is the 3 x 3 direction cosine matrix from the orbital frame to the body frame, and ω_{orb} is the orbital-frame rotation rate.

The quaternion-multiplication matrix is defined as:

$$\Omega(\omega) = \begin{bmatrix} 0 & -\omega_x & -\omega_y & -\omega_z \\ \omega_x & 0 & \omega_z & -\omega_y \\ \omega_y & -\omega_z & 0 & \omega_x \\ \omega_z & \omega_y & -\omega_x & 0 \end{bmatrix} \tag{9}$$

Aerodynamic torque

The aerodynamic torque arises from the interaction between the spacecraft and the incoming atmospheric flow. In the body-fixed coordinate system, the components of the aerodynamic torque are given by Eq. 10:

$$\vec{T}_a = \vec{r}_d \times \vec{a}_{drag} = \begin{vmatrix} \hat{\imath} & \hat{\jmath} & \hat{k} \\ x_d & y_d & z_d \\ a_x & a_y & a_z \end{vmatrix}, \vec{a}_{drag} = -\frac{1}{2} \cdot \frac{C_x S}{m} \rho v^2 \hat{e} \tag{10}$$

where $\vec{r}_d$ is the position vector from the satellite's center of mass to the center of pressure, v is the magnitude of the satellite's velocity relative to the atmosphere, and $\hat{e}$ is the unit vector in the direction of the velocity vector.

For nanosatellites shaped as rectangular parallelepipeds, the projected cross-sectional area is calculated as (Belokonov and Timbay 2020):

$$S = S_1 \cdot |\hat{v}_x| + S_2 \cdot |\hat{v}_y| + S_3 \cdot |\hat{v}_z| \tag{11}$$

where S_1, S_2, S_3 are the areas of the faces perpendicular to the satellite's body-fixed axes, and $\hat{v}_x, \hat{v}_y, \hat{v}_z$ are the projections of the unit vector of the relative velocity onto these axes.

Gravitational torque

When a spacecraft interacts with Earth's gravitational field, a gravity-gradient torque arises, given by:

$$\vec{T}_{grav} = 3\frac{\mu}{r^3}\vec{r} \times (\boldsymbol{I} \cdot \vec{r}), \tag{12}$$

where $\mu = 398.602\ km^3 \cdot s^{-2}$ is the Earth's gravitational parameter, $\vec{r}$ is the position vector from the spacecraft to Earth's center (expressed in the body-fixed coordinate system), r is the distance from the satellite to the Earth's center of mass, and $\boldsymbol{I}$ is the spacecraft's inertia tensor.

Magnetic damping torque

The damping torque generated by the interaction between the magnetic dipole moment of the hysteresis rod $\vec{m}_{hyst}$ and the geomagnetic field $\vec{B}$ is given by the vector cross product:

$$\vec{T}_{mag-damp} = \vec{m}_{hyst} \times \vec{B} \tag{13}$$

where $\vec{m}_{hyst} = \frac{B_{hyst}(H) \cdot V_{hyst}}{\mu_0}\left(k \cdot \hat{e}_{hyst_i}, k\hat{e}_{hyst_j} k\hat{e}_{hyst_k}\right)$, $B_{hyst}(H)$ is the magnetic flux induced in the rod, V_{hyst} the hysteresis rod's volume, $\mu_0 = 4\pi \cdot 10^{-7}\ T \cdot m \cdot A^{-1}$ is the vacuum magnetic permeability, k is the number of rods per axis, and $\hat{e}_{hyst}$ is the unit vector in the rod's direction.

The magnetic flux induced in the rod can be approximated by Eq. 14 (Gerhardt 2010):

$$B_{hyst}(H) = \frac{2}{\pi} B_s \operatorname{atan}\left[p\left(\frac{B_i}{\mu_0} \pm H_c\right)\right];\ p = \frac{1}{H_c}\tan\left(\frac{\pi B_r}{2B_s\mu'_{hyst}}\right) \tag{14}$$

where μ'_{hyst} is the rod's apparent relative permeability, p is a constant, specific to each material, and B_i is the intensity of the magnetic field across the i direction.

The sign preceding H_c in Eq. 14 accounts for the resistance of the hysteresis material to changes in the external magnetic field. Mathematically, this behavior is represented by changing the sign of H_c depending on whether the magnetic field intensity is increasing or decreasing. The sign of H_c is therefore determined by the sign of the time derivative of the local geomagnetic field:

$$H_c, if\frac{dB_i}{dt} < 0;\ -H_c, if\frac{dB_i}{dt} > 0 \tag{15}$$

For the most common hysteresis materials used in small satellite missions, empirical approximations for the true relative permeability of the rod μ_{hyst} can be found, and μ'_{hyst} can be calculated as:

$$\mu'_{hyst} = \frac{\mu_{hyst}}{1 + N \cdot \mu_{hyst}}, \tag{16}$$

with $N = \left(\frac{4l}{d\sqrt{\pi}} + 2\right)^{-1}$ being the demagnetisation factor, l the rod's length, and d its cross-sectional area. The distance between the rods also affects performance, but it is not considered in this work.

Simulation results and discussion

To evaluate the performance of passive magnetic damping in VLEO, three orbital scenarios were considered: (1) an equatorial orbit with 0° inclination; (2) a mid-inclination orbit at 72°; and (3) a Sun-synchronous orbit at 98°. These scenarios correspond to distinct geomagnetic environments, ranging from relatively weak and homogeneous fields (0°) to strong and rapidly varying mid-latitude fields (72°) and strong, highly variable high-latitude fields (98°).

Unless otherwise stated, all simulations were carried out using the same spacecraft configuration, hysteresis material, and initial angular velocities, presented in Table 2 (hereafter referred to as the "initial state").

Table 2. Initial conditions used for the simulation.

Spacecraft standard	CubeSat 3U
Center of mass offset relative to geometric center, m	$r_d = [0.0054 \quad 0 \quad -0.006]$
Initial angular velocity, $deg \cdot s^{-1}$	$\omega(0) = [4 \quad 4 \quad 4]$
Inertia tensor, $kg \cdot m^2$	$I = \begin{bmatrix} 0.0099 & -0.0001 & -0.0028 \\ -0.0001 & 0.0537 & 0.0001 \\ -0.0028 & 0.0001 & 0.0522 \end{bmatrix}$
Coercive force, $A \cdot m^{-1}$	$H_c = 1.5$
Remanent induction, T	$B_r = 1.69$
Saturation induction, T	$B_s = 0.73$
Rod dimensions, mm	85 x 2 x 1 (lenght x thicknes x swidth)
Rod configuration	2 rods along the spacecraft O_x and O_y axes

Source: Elaborated by the authors.

Figure 4 shows the time history of the angular velocity components during passive magnetic damping at 300 km, where damping occurred after approximately 43 h. The quantitative results for all simulated orbital scenarios, altitudes, and hysteresis configurations are summarized in Table 3, which reports the damping time and steady-state angular velocity amplitudes for each case.

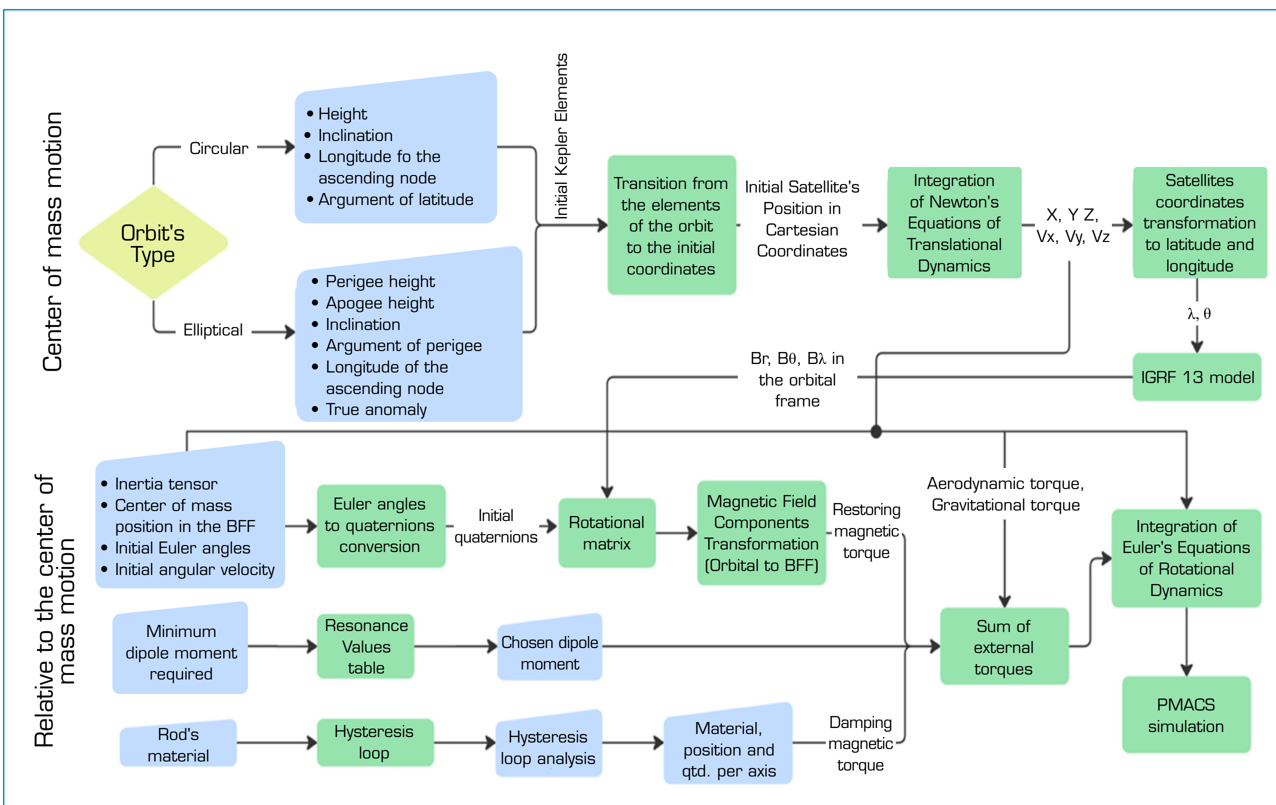

Source: Elaborated by the authors.

Figure 4. Workflow of the developed software implementing the methodology.

For equatorial orbits, the results in Table 3 show that damping is slower than for higher-inclination cases, which is consistent with the relatively weak geomagnetic field near the equator. At an altitude of 300 km, the angular velocity components reach the steady-state regime after approximately 46 h (Fig. 5), while at 500 km the damping time increases to about 58 h.

Table 3. Summary of angular velocity damping performance for different orbital inclinations and configurations.

Case	Altitude (km)	Inclination (degrees)	Hysteresis rods configuration	Damping time (h)	Steady-state angular velocity amplitude ($deg \cdot s^{-1}$)
1	300	0	Initial state	≈ 46	≈ 0.15
	500	0	Initial state	≈ 58	≈ 0.18
2	300	72	Initial state	≈ 41	≈ 0.14
	300	72	3 rods (1/axis)	≈ 32	≈ 0.10
3	300	98	3 rods (1/axis)	≈30	≈ 0.13
	300	98	3 rods (1/axis) Dimensions: 150 x 2 x 1	≈ 9	≈ 0.10

Source: Elaborated by the authors.

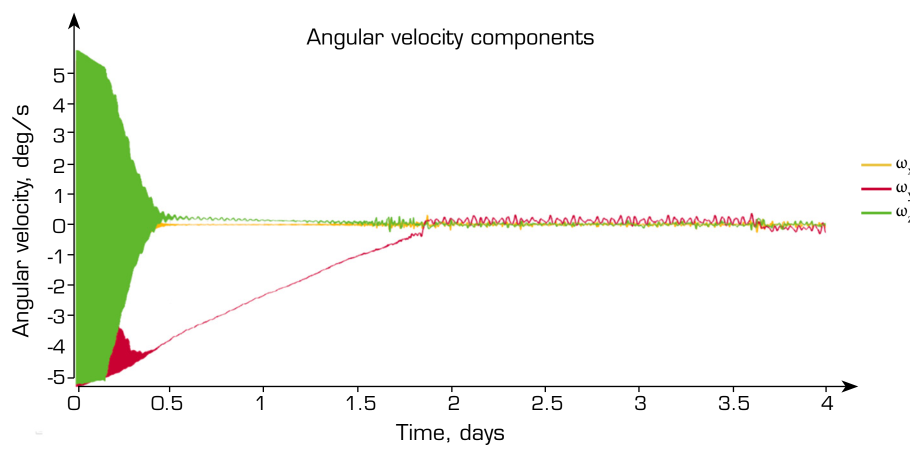

Source: Elaborated by the authors.

Figure 5. Damping effect at 300 km and inclination 0°.

For the mid-inclination case, the damping time does not decrease as much as might be expected relative to the equatorial case at the same altitude: the stabilization time is reduced by only about 5 h. One possible explanation is the saturation behavior of the hysteresis material. Since the rods have a finite saturation limit, their damping efficiency does not increase indefinitely with the magnitude of the external magnetic field. Once the field strength approaches the saturation region, further increases in lead only to marginal improvements in the generated damping torque.

If a damping time of around 40 h is considered too long for a particular mission, Table 3 also shows that configuration changes can be more effective than relying on inclination alone. For example, adding a third hysteresis rod along the axis leads to earlier damping.

Finally, for the Sun-synchronous case, damping remains comparable to the mid-inclination orbit despite the stronger geomagnetic environment, again suggesting saturation effects. However, when the same material and number of rods are retained, but the rod length is increased (from 8.5 cm to 15 cm), the damping performance significantly improves.

CONCLUSION

This paper presented the results obtained by applying a previously developed methodology for providing PMAC to nanosatellites equipped with hysteresis rods and operating in VLEO. Numerical simulations were carried out for three representative orbital scenarios using the same spacecraft physical parameters. In all cases, angular-velocity damping was achieved, demonstrating that, with appropriate sizing and placement of hysteresis rods, PMAC can stabilize angular motion in VLEO within acceptable timeframes.

As expected, damping in VLEO is faster than at higher altitudes due to the stronger geomagnetic field. Near-equatorial orbits exhibit less efficient damping because of the relatively weak magnetic field in these regions. Increasing the orbital inclination to 72° or 98° while maintaining the same PMAC configuration, however, does not lead to a proportional acceleration of damping, as the achievable performance is limited by the properties of the hysteresis material itself, such as saturation effects.

For the same material, the results show that, in the cases considered, damping performance improves when a third hysteresis rod is added along the remaining axis and improves further when the rod length is increased from 8.5 cm to 15 cm. Nevertheless, this should not be interpreted as a general rule. In previous missions, inappropriate layouts or excessive rod volume have even resulted in weaker-than-expected damping due to mutual interaction between magnetic materials or premature saturation (Farrahi and Sanz-Andrés 2013). This highlights the importance of tailoring the magnetic configuration to the specific spacecraft design and mission conditions, and of using simulation tools (such as the developed software) to predict attitude behavior, rather than assuming a linear correspondence between the number/size of rods and performance improvement.

The obtained results indicate the potential of using magnetic materials to stabilize angular oscillations in VLEO, rather than relying solely on geometric alternatives, deployable surfaces, or center-of-mass shifting. Future work will include incorporating a dynamic hysteresis model and developing more efficient numerical integration schemes to improve modelling accuracy under rapidly varying magnetic conditions in VLEO, as well as including permanent magnets to evaluate their contribution to pointing performance.

CONFLICTS OF INTEREST

Nothing to declare.

AUTHOR CONTRIBUTIONS

Conceptualization: Souza TOB and Lomaka IA; **Methodology:** Souza TOB and Lomaka IA; **Investigation:** Souza TOB and Lomaka IA; **Writing – Original Draft:** Souza TOB; **Writing – Review and Editing:** Lomaka IA; **Supervision:** Lomaka IA; **Final Approval:** Lomaka IA.

DATA AVAILABILITY STATEMENT

The data will be available upon request.

FUNDING

Russian Science Foundation
Grant No: 23-72-30002

DECLARATION OF USE OF ARTIFICIAL INTELLIGENCE TOOLS

The authors declare that no artificial intelligence tools were used in the preparation, analysis, or writing of this article.

ACKNOWLEDGEMENTS

The authors would like to acknowledge the financial support for the presented work provided by a research grant from the Russian Science Foundation as part of the project "Technologies for the Development of Small-Scale Space Systems for Geo- and Heliophysical Monitoring to Ensure the Safety of Space Activities and Support Ground Infrastructure." Author would also like to thank the team of the Interuniversity Department of Space Research for their assistance and support during this study.

REFERENCES

Afful MA (2014) Orbital lifetime predictions of Low Earth Orbit satellites and the effect of a DeOrbitSail (master's thesis). Stellenbosch: Stellenbosch University [accessed Oct 10 2025]. http://hdl.handle.net/10019.1/85862

Allasio A, Anselmi A, Catastini G, Cesare S, Dumontel M, Saponara M, Sechi G, Tramutola A, Vinai B, André G, Fehringer M (2010) GOCE mission: design phases and in-flight experiences. Adv Astronaut Sci 137:AAS 10-081. [accessed Nov 1 2025]. https://www.researchgate.net/publication/260920187_Goce_mission_Design_phases_and_in-flight_experiences

Aslan AR, Sofyali A, Umit E, Tola C (2011) TURKSAT-3USAT: a 3U communication CubeSat with passive magnetic stabilization. Paper presented 2011 5th International Conference on Recent Advances in Space Technologies. IEEE; Istanbul, Turkey. https://doi.org/10.1109/RAST.2011.5966949

Battagliere ML, Santoni F, Piergentili F, Ovchinnikov M, Graziani F (2010) Passive magnetic attitude stabilization system of the EduSAT microsatellite. Proc Inst Mech Eng G J Aerosp Eng 224(3):283-295. https://doi.org/10.1243/09544100JAERO732

Belokonov IV, Timbai IA (2020) Motion of a nanosatellite relative to the center of mass in Low Earth Orbits. Samara: Samara University Publishing House. (In Russian). [accessed Oct 1 2025]. https://repo.ssau.ru/handle/Uchebnye-izdaniya/Dvizhenie-nanosputnika-otnositelno-centra-mass-na-okolozemnyh-orbitah-ucheb-posobie-Tekst-elektronnyi-85067

Belokonov IV, Timbai IA, Davydov DD (2019) Passive stabilization systems for CubeSat nanosatellites: general principles and features. Paper presented 2019 26th Saint Petersburg International Conference on Integrated Navigation Systems. IEEE; St. Petersburg, Russia. https://doi.org/10.23919/ICINS.2019.8769434

BIS Research (2025) Very Low Earth Orbit (VLEO) satellite market set to reach $15025 million by 2034. [accessed Nov 1 2025]. https://bisresearch.com/insights/very-low-earth-orbit-vleo-satellite-market-set-to-reach-dollar15025-million-by-2034

Carletta S, Nascetti A, Matadha SSG, Iannascoli L, Albuquerque TB, Davis NM, Schirone L, Impresario G, Pirrotta S, Brucato JR (2022) Characterization and testing of the passive magnetic attitude control system for the 3U AstroBio CubeSat. Aerospace (Basel) 9(11):723. https://doi.org/10.3390/aerospace9110723

Crisp NH, Roberts PCE, Romano F, Smith KL, Oiko VTA, Sulliotti-Linner V, Hanessian V, Herdrich GH, García-Almiñana D, Kataria D, et al. (2021) System modelling of Very Low Earth Orbit satellites for Earth observation. Acta Astronaut. 187: 475-449. https://doi.org/10.1016/j.actaastro.2021.07.004

DISCOVERER (2025) DISCOVERER Project. [accessed Aug 20 2025]. https://discoverer.space/

Douglas ES, Tracy K, Manchester Z (2021) Practical limits on nanosatellite telescope pointing: the impact of disturbances and photon noise. Front Astron Space Sci 8:676252. https://doi.org/10.3389/fspas.2021.676252

Farrahi A, Sanz-Andrés A (2013) Efficiency of hysteresis rods in small spacecraft attitude stabilization. Int J Aerosp Eng 2013: 459573. https://doi.org/10.1155/2013/459573

Gerhardt D (2010) Passive magnetic attitude control for CubeSat spacecraft. Paper presented 2010 24th Annual AIAA/USU Conference on Small Satellites. AIAA/USU; Logan, USA.

Jiang Y, Zhang J, Tian P, Liang T, Li Z, Wen D (2023) Aerodynamic drag analysis and reduction strategy for satellites in very low Earth orbit. Aerosp Sci Technol 132:108077. https://doi.org/10.1016/j.ast.2022.108077

Ovchinnikov MYu (2012) Attitude dynamics of a small-sized satellite equipped with hysteresis damper. Adv Astronaut Sci 145:311-330. [accessed Oct 10 2025]. https://www.researchgate.net/publication/275856723_Attitude_dynamics_of_a_small-sized_satellite_equipped_with_hysteresis_damper

Ovchinnikov MYu, Penkov VI (2002) Passive magnetic attitude control system for the Munin nanosatellite. Cosmic Res 40(2):142-156. https://doi.org/10.1023/A:1015197303662

Rawashdeh SA (2010) Passive attitude stabilization for small satellites (master's thesis). Lexington: University of Kentucky. [accessed Nov 1 2025]. https://uknowledge.uky.edu/cgi/viewcontent.cgi?referer=&httpsredir=1&article=1628&context=gradschool_theses

Romano F, Espinosa-Orozco J, Pfeiffer M, Herdrich G, Garcia-Almiñana D (2021) Intake design for an atmosphere-breathing electric propulsion system (ABEP). Acta Astronaut. 187:225-235. https://doi.org/10.1016/j.actaastro.2021.06.033

Santoni F, Zelli M (2009) Passive magnetic attitude stabilization of the UNISAT-4 microsatellite. Acta Astronaut 65(5-6): 792-803. https://doi.org/10.1016/j.actaastro.2009.03.012

Sizov D, Aslanov V (2024) Attitude dynamics of small magnetic axisymmetric satellites in near-equatorial low Earth orbits/very low Earth orbits. J Guid Control Dyn47(12). https://doi.org/10.2514/1.G008393

Souza TO, Lomaka IA (2024) Methodology and dedicated software development to provide passive magnetic attitude control for CubeSats. Paper presented 2024 IAF Astrodynamics Symposium, 75th International Astronautical Congress. IAF; Milan, Italy. [accessed Nov 10 2025]. https://doi.org/10.52202/078368-0090

Virgili-Llop J, Polat HC, Romano M (2019) Attitude stabilization of spacecraft in Very Low Earth Orbit by center-of-mass shifting. Front Robot AI 6:7. https://doi.org/10.3389/frobt.2019.00007

Walsh J, Berthoud L, Allen C (2021) Drag reduction through shape optimisation for satellites in Very Low Earth Orbit. Acta Astronaut 179:105-121. https://doi.org/10.1016/j.actaastro.2020.09.018